Available online at www.sciencedirect.com
SCIENCE DIRECT®
Journal of Solid State Chemistry 178 (2005) 2067–2076
JOURNAL OF SOLID STATE CHEMISTRY
www.elsevier.com/locate/jssc

Synthesis and nonlinear optical properties of $BaTi(BO_3)_2$ and $Ba_3Ti_3O_6(BO_3)_2$ crystals in glasses with high TiO_2 contents

Shinji Kosaka[a], Yasuhiko Benino[a], Takumi Fujiwara[a], Vesselin Dimitrov[b], Takayuki Komatsu[a,*]

[a]*Department of Chemistry, Nagaoka University of Technology, 1603-1Kamitomioka-cho, Nagaoka 940-2188, Japan*
[b]*Department of Silicate Technology, University of Chemical Technology and Metallurgy, 8 Kl, Ohridki Blvd., Sofia 1756, Bulgaria*

Received 8 March 2005; received in revised form 18 April 2005; accepted 19 April 2005

Abstract

The ternary $BaO–TiO_2–B_2O_3$ glasses containing a large amount of TiO_2 (20–40 mol%) are prepared, and their optical basicities (Λ), the formation, structural features and second-order optical nonlinearities of $BaTi(BO_3)_2$ and $Ba_3Ti_3O_6(BO_3)_2$ crystals are examined to develop new nonlinear optical materials. It is found that the glasses with high TiO_2 contents of 30–40 mol% show large optical basicities of $\Lambda = 0.81-0.87$, suggesting the high polarizabity of TiO_n polyhedra ($n = 4-6$) in the glasses. $BaTi(BO_3)_2$ and $Ba_3Ti_3O_6(BO_3)_2$ crystals are found to be formed as main crystalline phases in the glasses. It is found that $BaTi(BO_3)_2$ crystals tend to orient at the surface of crystallized glasses. The new XRD pattern for the $Ba_3Ti_3O_6(BO_3)_2$ phase is proposed through Rietvelt analysis. The second harmonic intensities of crystallized glasses were found to be 0.8 times as large as α-quartz powders, i.e., $I^{2\omega}(\text{sample})/I^{2\omega}(\alpha-\text{quartz}) = 0.8$, for the sample with $BaTi(BO_3)_2$ crystals and to be $I^{2\omega}(\text{sample})/I^{2\omega}(\alpha-\text{quartz}) = 68$ for the sample with $Ba_3Ti_3O_6(BO_3)_2$ crystals. The Raman scattering spectra for these two crystalline phases are measured for the first time and their structural features are discussed.

Keywords: Glass; Electronic polarizability; Nonlinear optical crystals; $BaTi(BO_3)_2$; $Ba_3Ti_3O_6(BO_3)_2$; Raman scattering spectra; Crystallized glass

1. Introduction

Crystallized glasses consisting of nonlinear optical crystals have received much interest, because such materials have a high potential for laser host, tunable waveguide, tunable fiber grating, and so on. For instance, crystallized glasses consisting of $LaBGeO_5$, $SrBi_2Ta_2O_9$ and $Ba_2TiGe_2O_8$ which are noble optical nonlinear and ferroelectric crystals have been fabricated [1–5]. In particular, it should be pointed out that the optical second-order nonlinearity of d_{33} for ferroelectric $Ba_2TiGe_2O_8$ crystals in transparent crystallized glasses is 10–20 pm/V, being comparable to the d_{22} and d_{11} values of $LiNbO_3$ single crystal [4,5]. Very recently, Park et al. [6] reported a new barium titanium oxoborate crystal of $Ba_3Ti_3O_6(BO_3)_2$ and found that the second harmonic generation (SHG) efficiency of this crystal is equal to 95% of that of $LiNbO_3$.

On the other hand, it is well known that the system of $BaO–TiO_2–B_2O_3$ exhibits an extremely large glass-forming region, in which glasses containing a large amount of TiO_2, up to 50 mol%, are formed [7]. Bhargava et al. [8] examined the crystallization behavior of various glasses in the system of $BaO–TiO_2–B_2O_3$, but in their study, the formation of $Ba_3Ti_3O_6(BO_3)_2$ crystals has not been reported. It should be also pointed out that the glasses containing a large amount of TiO_2 show large third-order optical nonlinearities [9,10], suggesting that the polarizability of Ti–O bonds in glass might be high. Adair et al. [11] demonstrated that TiO_2 shows the highest nonlinear refractive index in a large number of

*Corresponding author. Fax: +81 258 47 9300.
E-mail address: komatsu@chem.nagaokaut.ac.jp (T. Komatsu).

0022-4596/$ - see front matter © 2005 Elsevier Inc. All rights reserved.
doi:10.1016/j.jssc.2005.04.023

optical crystals, indicating a very high oxygen hyperpolarizability of Ti–O pairs. Recently, Kityk et al. [12] proposed that 2*p*O(oxygen)–3*d*Ti chemical bonds play crucial role in the observed polarizabilities of Ti–O clusters such as TiO_4 in $Bi_{12}TiO_{20}$ nanocrystals incorporated into matrices. It is, therefore, of interest and of importance to clarify the electronic polarizability and crystallization behavior of glasses with high TiO_2 contents such as $BaO–TiO_2–B_2O_3$ and to develop new crystallized glasses showing excellent nonlinear optical properties. In this study, we examined electronic polarizabilities (optical basicity) of precursor glasses, crystalline phases, and second harmonic (SH) intensities of crystallized samples in the ternary $BaO–TiO_2–B_2O_3$ glasses containing a large amount of TiO_2 (30–40 mol%). In particular, we focused our attention on two crystalline phases of $BaTi(BO_3)_2$ and $Ba_3Ti_3O_6(BO_3)_2$. We clarified for the first time that $Ba_3Ti_3O_6(BO_3)_2$ crystals showing large SH intensities are formed in the crystallized glasses with high TiO_2 contents and $BaTi(BO_3)_2$ crystals exhibit a second-order optical nonlinearity. Furthermore, the new X-ray diffraction (XRD) pattern for the $Ba_3Ti_3O_6(BO_3)_2$ phase was proposed through Rietvelt analysis. The Raman scattering spectra for these two crystalline phases were also measured for the first time in this study.

2. Experimental

Glasses in the ternary system of $BaO–TiO_2–B_2O_3$ were prepared by using a conventional melt-quenching method. Commercial powders of reagent-grade BaO, TiO_2, and B_2O_3 were mixed together and melted in a platinum crucible at 1200–1300 °C for 1 h in an electric furnace. The melts were poured onto an iron plate and pressed to a thickness of 1–1.5 mm by another iron plate. Glass transition T_g and crystallization peak T_p temperatures were determined using differential thermal analyses (DTA) at a heating rate of 10 K/min. Densities of glasses were determined with the Archimedes method using distilled water as an immersion liquid. Refractive indices at a wavelength of 632.8 nm (He–Ne laser) were measured at room temperature with an ellipsometer (Mizojiri Optical, DVA-36 model).

In order to determine crystalline phases formed by crystallization, plate-shape glasses were pulverized and heat-treated at some temperatures. By using powdered glasses, fully crystallized glasses were obtained. For the fabrication of transparent crystallized glasses, well-polished plate-shape (bulk) glasses were used. As will be shown in the next section, $BaO–TiO_2–B_2O_3$ glasses with high TiO_2 contents tend to show surface crystallization. Crystalline phases present in the heat-treated powdered and bulk samples were examined by XRD analysis at room temperature using Cu*K*α radiation and from Raman scattering spectra (Tokyo Instruments Co., Nanofinder operated at Ar^+ (488 nm) laser). SH intensities of crystallized powders with particle sizes of 32–45 μm were evaluated using the Kurtz powder method [13]. A fundamental wave of a Q-switch Nd:YAG laser operating at a wavelength of $\lambda = 1064$ nm was used as the incident light. The SH intensity of α-quartz powders with a particle size of 20–25 μm was used as a reference.

3. Results and discussion

3.1. DTA study of glasses

The glass nominal compositions in the $BaO–TiO_2–B_2O_3$ system examined in the present study are given in Table 1. Water contents in these glasses have not been determined. DTA curves for some glasses are shown in Fig. 1, giving the peaks due to the glass transition,

Table 1
Chemical compositions, glass transition temperature T_g, and crystallization peak temperature T_p, density d, and refractive index n of $BaO–TiO_2–B_2O_3$ glasses. The main crystalline phases in the samples obtained by heat-treatment at T_p for 3 h are given

Glass composition (mol%)				T_g(°C)	T_p(°C)	D (g/cm^3)	n	Crystalline phases
Sample	BaO	TiO_2	B_2O_3					
#1	20	20	60	568	614	3.15	1.634	β-BaB_2O_4
#2	30	20	50	588	791	3.68	1.718	$BaTi(BO_3)_2$
#3	40	20	40	567	731	4.08	1.751	β-BaB_2O_4, $BaTi(BO_3)_2$
#4	50	20	30	500	620	4.43	1.751	β-BaB_2O_4
#5	30	30	40	586	728	3.85	1.801	$BaTi(BO_3)_2$, $Ba_3Ti_3O_6(BO_3)_2$
#6	40	30	30	558	709	4.20	1.827	$BaTi(BO_3)_2$, β-BaB_2O_4
#7	33.3	33.3	33.3	580	749	4.09	1.847	$BaTi(BO_3)_2$
#8	35	35	30	582	748	4.17	1.861	$BaTi(BO_3)_2$, $Ba_3Ti_3O_6(BO_3)_2$
#9	37.5	37.5	25	572	725	4.31	1.865	$BaTi(BO_3)_2$, $Ba_3Ti_3O_6(BO_3)_2$
#10	40	40	20	554	712	4.37	1.884	$BaTi(BO_3)_2$, $Ba_3Ti_3O_6(BO_3)_2$
#11[a]	36	48	16	582	702	4.32	1.931	$BaTi(BO_3)_2$, $Ba_3Ti_3O_6(BO_3)_2$

[a]Partially crystallized.

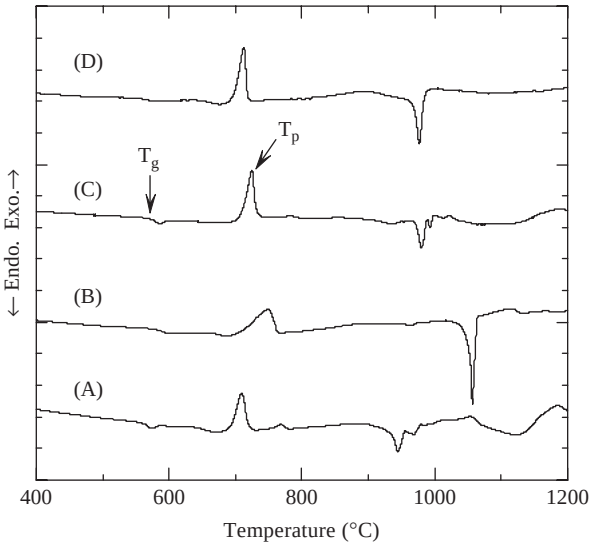

Fig. 1. DTA patterns for bulk glasses: (A) $40BaO \cdot 30TiO_2 \cdot 30B_2O_3$, (B) $33.3BaO \cdot 33.3TiO_2 \cdot 33.3B_2O_3$, (C) $37.5BaO \cdot 37.5TiO_2 \cdot 25B_2O_3$ and (D) $40BaO \cdot 40TiO_2 \cdot 20B_2O_3$. Heating rate was 10 K/min. T_g and T_p are the glass transition and crystallization peaks temperatures, respectively.

crystallization, and melting. The melt-quenched sample with the composition of $33.3BaO \cdot 33.3TiO_2 \cdot 33.3B_2O_3$ corresponding to $BaTi(BO_3)_2$ was the glassy state and gives the values of $T_g = 580\,^{\circ}C$ and $T_p = 749\,^{\circ}C$. As seen in Fig. 1, however, the exothermic peak due to the crystallization is broad, and the crystallization starts near 700 °C. On the other hand, the sample with the composition of $42 \cdot 5BaO \cdot 42 \cdot 5TiO_2 \cdot 15B_2O_3$ corresponding to $Ba_3Ti_3O_6(BO_3)_2$ was crystallized. The values of T_g and T_p for the glasses determined from DTA curves are summarized in Table 1, giving the values of $T_g = 500-588\,^{\circ}C$ and $T_p = 614-790\,^{\circ}C$. It should be pointed out that the glasses containing TiO_2 contents of 30–48 mol% show similar glass transition temperatures of ~570 °C and similar crystallization peak temperatures of ~720 °C, irrespective of TiO_2 content. The values of density d and refractive index n are also given in Table 1. It is seen that both values increase with the substitution of TiO_2 for B_2O_3. For example, $33.3BaO \cdot 33.3TiO_2 \cdot 33.3B_2O_3$ glass has the values of $d = 4.09\,g/cm^3$ and $n = 1.85$.

3.2. Eelectronic polarizability of glasses

One of the most important properties of materials, which is closely related to their applicability in the field of optics and electronics, is the electronic polarizability. It is of particular interest and of importance to examine the electronic polarizability of glasses with high TiO_2 contents. Estimation of the state of polarizability of the ions is the subject of the so-called polarizability approach based on the Lorentz–Lorenz equation giving the relationship between molar refraction R_m and refractive index n:

$$R_m = \left[\frac{(n^2-1)}{(n^2+2)}\right]\left(\frac{M}{d}\right) = \left[\frac{(n^2-1)}{(n^2+2)}\right]V_m = \frac{4\pi\alpha_m N}{3}, \quad (1)$$

where M is the molecular weight, d the density, V_m the molar volume, α_m the molar polarizability, and N the Avogadro's number. This equation gives the average molar refraction for isotropic substances such as liquids, glasses and cubic crystals. The Lorentz–Lorenz equation allows calculating the so-called electronic polarizability of oxide ions, $\alpha_{O^{2-}}(n)$, in oxide materials by subtracting the cation polarizability from the molar polarizability, α_m, taking into account the relationship proposed by Dimitrov and Sakka [14] for simple oxides and successfully applying for various oxide glasses [15–17]:

$$\alpha_{O^{2-}}(n) = \left[\frac{R_m}{2.52} - \Sigma\alpha_i\right](N_{O^{2-}})^{-1} \quad (2)$$

where $\Sigma\alpha_i$ denotes molar cation polarizability and $N_{O^{2-}}$ denotes the number of oxide ions in the chemical formula. Furthermore, as discussed by Duffy [18], an intrinsic relationship exists between electronic polarizability of the oxide ions and so-called optical bacisity of the oxide medium, Λ, as given by

$$\Lambda = 1.67\left(1 - \frac{1}{\alpha_{O^{2-}}}\right). \quad (3)$$

This relation presents a general trend toward an increase in the oxide ion polarizability with increasing optical basicity. The optical basicity of an oxide medium as proposed by Duffy and Ingram [19,20] is a numerical expression of the average electron donor power of the oxide species constituting the medium, and thus it is used as a measure of the acid–base properties of oxides, glasses, alloys, slags, molten salts, etc. According to the pioneering work of Duffy and Ingram [19,20], the optical basicity of glasses can be determined experimentally from frequency shifts observed in the $^1S_0 \rightarrow {}^3P_1$ band in UV spectra of probe ions such as Tl^+, Pb^{2+}, or Bi^{3+} with s^2 electron configuration incorporated in the glass matrix. A new step in the development of experimental techniques for direct estimation of optical basicity seems to be X-ray photoelectron spectroscopy (XPS). Recently, the O 1s chemical shift in XPS spectra was used intensively for the search of an adequate relation between the peak position and optical basicity of oxides and glasses [21–25]. Since increased oxide ion polarizability means stronger electron donor ability of oxide ions, the physical background of the oxide ion polarizability and optical basicity is naturally the same.

Using Eqs. (1), (2), and (3), we estimated the values of α_m, $\alpha_{O^{2-}}$ and Λ of $BaO–TiO_2–B_2O_3$ glasses prepared in the present study, and the results are shown in Table 2

Table 2
Molar volume V_m, molar polarizability α_m, electronic polarizability of oxide ions $\alpha_{O^{2-}}$, and optical basicity Λ of $BaO–TiO_2–B_2O_3$ glasses

Sample	V_m (cm^3/mol)	α_m ($Å^3$)	$\alpha_{O^{2-}}$ ($Å^3$)	Λ
#1	28.07	3.979	1.510	0.564
#2	26.30	4.109	1.634	0.648
#3	25.75	4.163	1.745	0.713
#4	25.64	4.145	1.841	0.763
#5	25.41	4.310	1.799	0.742
#6	25.25	4.384	1.944	0.811
#7	24.63	4.351	1.883	0.783
#8	24.59	4.395	1.936	0.807
#9	24.35	4.367	1.975	0.824
#10	24.51	4.464	2.087	0.870
#11[a]	24.20	4.571	2.173	0.902

[a]Partially crystallized.

together with the value of V_m. The data on the cation polarizability of Ba^{2+}, Ti^{4+} and B^{3+} are taken from Ref. [14], i.e., $\alpha_{Ba^{2+}} = 1.595$, $\alpha_{Ti^{4+}} = 0.184$, and $\alpha_{Ba^{3+}} = 0.002\,Å^3$. As seen in Table 2, in particular, the glasses with high TiO_2 contents of 30–40 mol% show the electronic polarizabilities of $\alpha_{O^{2-}} = 1.95 - 2.09\,Å^3$ and the optical basicities of $\Lambda = 0.81 - 0.87$. These relatively large values suggest that $BaO–TiO_2–B_2O_3$ glasses with high TiO_2 contents have a high potential as nonlinear optical materials. The values of the optical basicity of TiO_2-based glasses such as $K_2O–TiO_2$ and $PbO–TiO_2$ have been reported to be $\Lambda = 0.85 - 1.17$ [15].

The electronic polarizability of oxide ions and optical basicity in $BaO–TiO_2–B_2O_3$ glasses increase with the increase of BaO and TiO_2 contents or with the decrease of B_2O_3 content. As reported by Dimitrov and Sakka [14], the simple oxides of BaO, TiO_2, and B_2O_3 have the following values: $\alpha_{O^{2-}} = 3.652\,Å^3$ and $\Lambda = 1.21$ for BaO, $\alpha_{O^{2-}} = 2.368\,Å^3$ and $\Lambda = 0.96$ for TiO_2 (rutile), $\alpha_{O^{2-}} = 1.945\,Å^3$ and $\Lambda = 0.43$ for B_2O_3. That is, the degree of basicity (electron donor ability of oxide ions) in simple oxides of BaO, TiO_2, and B_2O_3 is in the order of $B_2O_3 \ll TiO_2 < BaO$. The general trend that the electronic polarizability of oxide ions in $BaO–TiO_2–B_2O_3$ glasses increases largely with the substitution of BaO or TiO_2 for B_2O_3 seems, therefore, to be reasonable. Dimitrov and Komatsu [16,17] applied the interaction parameter A proposed by Yamashita and Kurosawa [26] to describe the polarizability state of an average oxide ion in numerous simple oxides and binary oxide glasses and its ability to form an ionic–covalent bond with the cation. The interaction parameter is a quantitative measure for the interionic interaction of negative ions such as O^{2-} with the nearest neighbors (cations). They proposed the following values: $A = 0.003\,Å^3$ for BaO, $A = 0.081\,Å^3$ for TiO_2, and $A = 0.244\,Å^3$ for B_2O_3. The increase in polarizability of the oxide ion as well as optical basicity of simple oxide or oxide glasses could be explained with decreased interaction inside the ionic pair, resulting in a smaller overlap between oxygen $2p$ and cation valence orbitals to form a chemical bond [16,17,27]. That is, the concept of interaction parameter suggests that the bonds of Ba–O and Ti–O are more ionic compared with B–O bond [27,28]. The general trend on the electronic polarizability of oxide ions observed in $BaO–TiO_2–B_2O_3$ glasses (Table 2) is also supported from the consideration of interaction parameters of BaO, TiO_2, and B_2O_3 oxides. Considering the above, it is expected that $BaO–TiO_2–B_2O_3$ glasses with high TiO_2 contents would show relatively large third-order optical nonlinearities [15].

3.3. Raman scattering spectra of glasses

The Raman scattering spectra at room temperature for some glasses including $33BaO \cdot 33TiO_2 \cdot 33B_2O_3$ (Sample #7) and $40BaO \cdot 40TiO_2 \cdot 20B_2O_3$ (Sample #10) are shown in Fig. 2. In the apparatus used in this study, the Raman scattering intensity at the wavenumber of below $300\,cm^{-1}$ cannot be measured because of the use of an edge filter. All glasses show broad peaks at 600–900 cm^{-1}. The Raman scattering spectra for $BaO–TiO_2–B_2O_3$ glasses have been reported by Bhargava et al. [29], giving similar Raman spectra for the glasses with 30–40 mol% TiO_2. They proposed that in the glasses with high TiO_2 contents Ti^{4+} ions enter the network structure and Ti–O–B linkages are formed. The

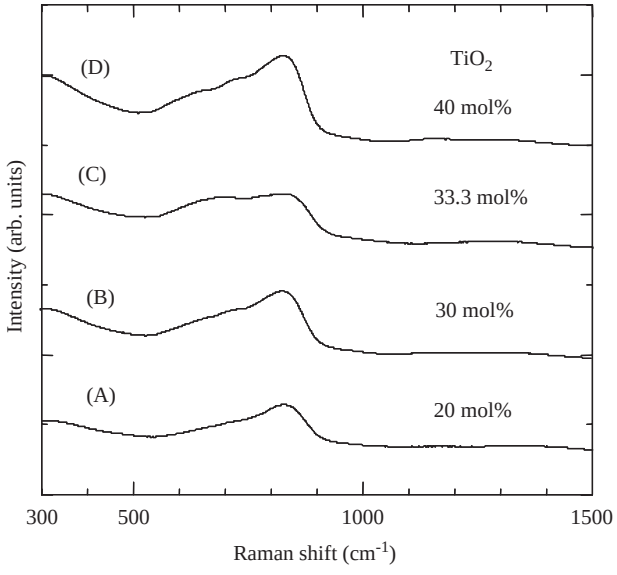

Fig. 2. Raman scattering spectra at room temperature for the glasses: (A) $40BaO \cdot 20TiO_2 \cdot 40B_2O_3$, (B) $40BaO \cdot 30TiO_2 \cdot 30B_2O_3$, (C) $33.3BaO \cdot 33.3TiO_2 \cdot 33.3B_2O_3$ and (D) $40BaO \cdot 40TiO_2 \cdot 20B_2O_3$.

Raman scattering spectra for some glasses containing TiO_2 such as K_2O–TiO_2 and Li_2O–TiO_2–SiO_2 have been reported by several authors so far [30–35], and it has been assigned that the peaks at 700–800 cm^{-1} correspond to Ti–O stretching vibration of TiO_4 tetrahedra and those at 550–700 cm^{-1} correspond to Ti–O stretching vibration of TiO_6 octahedra. As seen in Fig. 2, the relative peak intensity at ~620 cm^{-1} for the glasses with TiO_2 contents of 30–40 mol% such as $33.3BaO \cdot 33.3TiO_2 \cdot 33.3B_2O_3$ and $40BaO \cdot 40TiO_2 \cdot 30B_2O_3$ is much large compared with $40BaO \cdot 20TiO_2 \cdot 40B_2O_3$ with 20 mol% TiO_2. This might suggest the formation of TiO_6 octahedra in the glasses with high TiO_2 contents. It should be, however, pointed out that the Raman scattering spectra indicate the formation of both TiO_4 tetrahedra and TiO_6 octahedra in the glasses with high TiO_2 contents of 20–40 mol%. As discussed by Bhargava et al. [29], some borate structures such as pyroborate-type linkages give Raman scattering spectra in the range of 500–900 cm^{-1}. The detailed analysis of Raman scattering spectra would be needed to clarify the structure of BaO–TiO_2–B_2O_3 glasses. The structure of BaO–TiO_2–B_2O_3 glasses will be again discussed in the next section.

3.4. Structural features of $BaTi(BO_3)_2$ and $Ba_3Ti_3O_6(BO_3)_2$ crystals

As crystalline phases contains all kinds of cations Ba^{2+}, Ti^{4+}, and B^{3+} in the ternary system of BaO–TiO_2–B_2O_3, two crystalline phases of $BaTi(BO_3)_2$ and $Ba_3Ti_3O_6(BO_3)_2$ have been reported [6,36]. Prior to showing the results on the crystallization behavior of BaO–TiO_2–B_2O_3 glasses, it would be of worth to clarify the structural features of $BaTi(BO_3)_2$ and $Ba_3Ti_3O_6(BO_3)_2$ crystals. The structure of $BaTi(BO_3)_2$ crystal has been reported by Zhang et al. [36]: it has a rhombohedral system with the space group R-3, the lattice parameters are $a = 0.50205$ nm and $c = 1.63844$ nm, and the structure consists of BaO_6, TiO_6, and BO_3 units. The structure of $Ba_3Ti_3O_6(BO_3)_2$ has been clarified by Park et al. [6]; it has a hexagonal system with the space group $P\bar{6}2m$ (noncentrosymmetric), the lattice parameters are $a = 0.87377$ nm and $c = 0.39147$ nm, and the structure consists of BaO_{13}, TiO_6, BO_3 units. Park et al. [6] also reported that $Ba_3Ti_3O_6(BO_3)_2$ crystals show a very strong SH intensity, being equal to 95% of that of $LiNbO_3$.

The power XRD patterns for $BaTi(BO_3)_2$ and $Ba_3Ti_3O_6(BO_3)_2$ polycrystalline samples prepared by a solid-state reaction in the present study are shown in Figs. 3 and 4. $BaTi(BO_3)_2$ samples were prepared by a sintering of the mixture of oxides ($BaO:TiO_2:B_2O_3 = 1:1:1$) at 820 °C for 24 h in air, and $Ba_3Ti_3O_6(BO_3)_2$ samples were prepared by a sintering of the mixture ($BaO:TiO_2:B_2O_3 = 3:3:1.2$, e.g., 20% excess B_2O_3) at 920°C for 60 h in air. The 20% excess B_2O_3 was added because of the vaporization of B_2O_3 during sintering at a high temperature of 920 °C [6]. The XRD pattern for $BaTi(BO_3)_2$ crystals shown in Fig. 3 is consistent with that in JCPDS no.35-825. As pointed out by Park et al. [6], the compound previously reported as $Ba_2Ti_2B_2O_9$ [36] has been reformulated as $Ba_3Ti_3O_6(BO_3)_2$. The XRD pattern (JCPDS no.40-632) for $Ba_2Ti_2B_2O_9$ crystals has been reported by Millet et al.

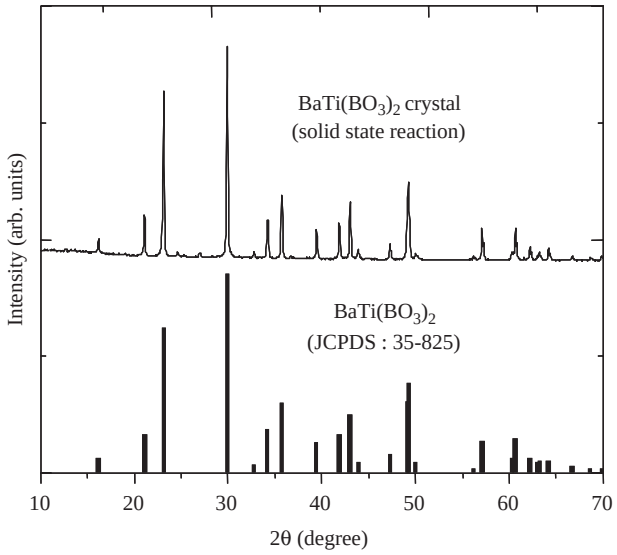

Fig. 3. Powder XRD pattern at room temperature for $BaTi(BO_3)_2$ crystals prepared by the solid-state reaction (820 °C, 24 h).

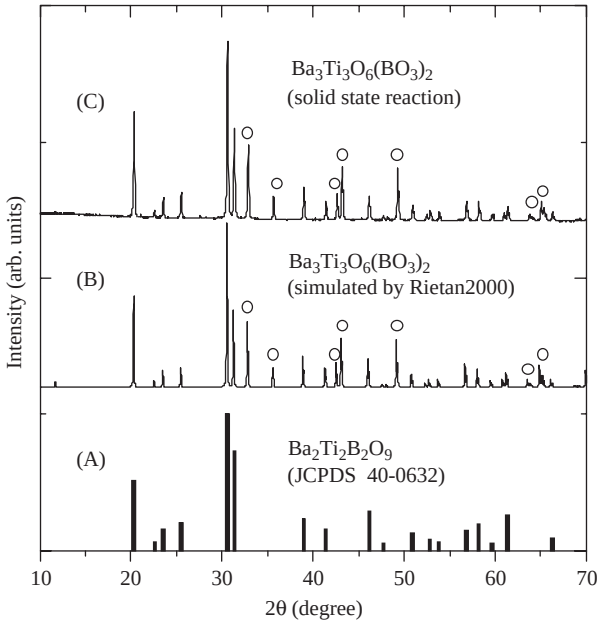

Fig. 4. Powder XRD pattern at room temperature for $Ba_3Ti_3O_6(BO_3)_2$ crystals prepared by the solid-state reaction (920 °C, 60 h). The pattern B is the simulated XRD pattern using Rietan 2000. The open circles (O) indicate the inconsistent peaks between the simulated XRD pattern and JCPDS 40-0632.

[37], and the data is shown in Fig. 4. As seen in Fig. 4, however, the XRD pattern for $Ba_3Ti_3O_6(BO_3)_2$ crystals prepared in the present study is not consistent with that reported by Millet et al. In Fig. 4, the inconsistent peaks are marked by open circles. We simulated the XRD pattern for $Ba_3Ti_3O_6(BO_3)_2$ polycrystalline powders using the structural information reported by Park et al. [6] and Rietan 2000 [38], and consequently, we found that some peaks are missing in the XRD pattern reported by Millet et al. [37]. The simulated and experimental XRD data for $Ba_3Ti_3O_6(BO_3)_2$ polycrystalline powders, e.g., the miller index, peak position, and peak intensity, are summarized in Table 3. Our simulation of the structure of $Ba_3Ti_3O_6(BO_3)_2$ crystals give the lattice parameters of $a = 0.8679(3)$ nm and $c = 0.3915(7)$ nm.

The SH intensities of $BaTi(BO_3)_2$ and $Ba_3Ti_3O_6(BO_3)_2$ polycrystalline samples were measured using the Kurtz powder method [13]. It was found that $Ba_3Ti_3O_6(BO_3)_2$ polycrystalline samples show a very strong SH intensity of approximately 60 times as large as α-quartz powders, i.e., $I^{2\omega}$(sample)/ $I^{2\omega}$(α–quartz) = 60, meaning that $Ba_3Ti_3O_6(BO_3)_2$ is an interesting nonlinear optical crystal as reported already by Park et al. [6]. It was found in the present study that $BaTi(BO_3)_2$ is also a nonlinear optical crystal having the SH intensity of approximately $I^{2\omega}$(sample)/$I^{2\omega}$(α–quartz) = 0.6. The results that both, $BaTi(BO_3)_2$ and $Ba_3Ti_3O_6(BO_3)_2$, are nonlinear optical crystals, would give us a high motivation to study the crystallization in $BaO–TiO_2–B_2O_3$ glasses with high TiO_2 contents.

The Raman scattering spectra for $BaTi(BO_3)_2$ and $Ba_3Ti_3O_6(BO_3)_2$ polycrystalline samples prepared by solid-state reactions in the present study are shown in Fig. 5. There has been no report on the Raman scattering spectra for these crystals. Considering various Raman scattering spectra for TiO_2–based compounds reported so far [30–33], the peaks at the wavenumber of below 650 cm^{-1} are associated with T–O vibrations in TiO_6 octahedral units. That is, the peaks at 200–400 cm^{-1} is due to O–Ti–O bending vibrations and the peaks at around 610 cm^{-1} is associated with Ti–O symmetric stretching vibrations. As can be seen in Fig. 5, $BaTi(BO_3)_2$ has a peak at 619 cm^{-1} and with a weak intensity, but $Ba_3Ti_3O_6(BO_3)_2$ shows a very strong peak at 625 cm^{-1}. Park et al. [6] reported that the TiO_6

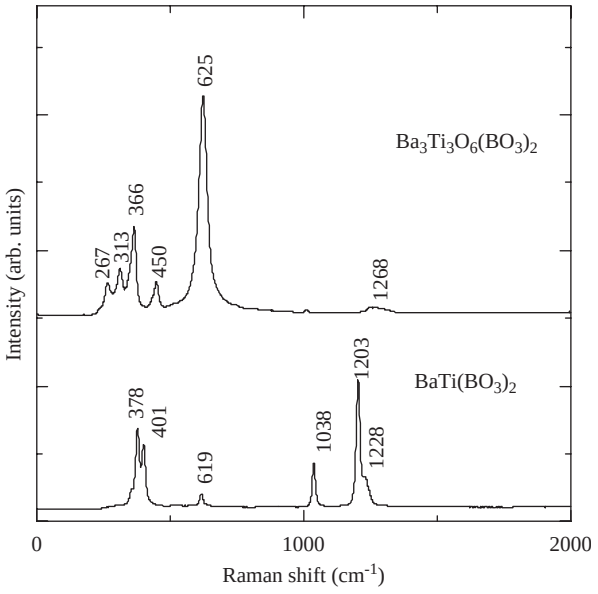

Fig. 5. Raman scattering spectra at room temperature for $BaTi(BO_3)_2$ and $Ba_3Ti_3O_6(BO_3)_2$ crystals prepared by the solid-state reaction.

Table 3
Indexed X-ray diffraction powder pattern for the $Ba_3Ti_3O_6(BO_3)_2$ phase

d_{obs}	hkl	$2\theta_{obs}$	$2\theta_{cal}$	I/I_0 (obs)	d_{obs}	hkl	$2\theta_{obs}$	$2\theta_{cal}$	I/I_0 (obs)
7.56	1 0 0	11.70	11.71	1.4	1.73	3 2 0	52.84	52.84	6.0
4.36	1 1 0	20.36	20.36	59.7	1.70	4 0 1	53.86	53.87	4.9
3.93	0 0 1	22.60	22.60	4.4	1.62	2 1 2	56.86	56.86	10.8
3.77	2 0 0	23.56	23.56	11.5	1.58	3 2 1	58.18	58.19	11.2
3.48	1 0 1	25.54	25.53	14.7	1.55	3 0 2	59.66	59.67	3.5
2.92	1 1 1	30.62	30.61	100.0	1.52	4 1 1	60.96	60.96	4.1
2.85	2 1 0	31.34	31.34	50.6	1.51	5 0 0	61.38	61.39	7.9
2.72	2 0 1	32.88	32.88	42.0	1.46	2 2 2	63.76	63.74	3.3
2.52	3 0 0	35.66	35.66	13.4	1.45	3 3 0	64.08	64.07	2.5
2.31	2 1 1	38.98	38.99	18.7	1.43	3 1 2	65.06	65.06	10.7
2.18	2 2 0	41.42	41.42	10.2	1.43	4 2 0	65.38	65.39	6.6
2.12	3 0 1	42.64	42.64	14.6	1.41	5 0 1	66.28	66.29	4.7
2.09	3 1 0	43.18	43.19	30.0	1.36	5 1 0	69.26	69.28	1.3
1.96	0 0 2	46.16	46.16	13.8	1.34	4 2 1	70.14	70.15	9.9
1.91	2 2 1	47.68	47.70	2.4	1.30	3 2 2	72.76	72.75	2.9
1.89	4 0 0	48.20	48.20	1.5	1.25	1 1 3	75.78	75.77	3.1
1.85	3 1 1	49.30	49.29	29.2	1.24	4 3 0	77.02	77.00	1.9
1.79	1 1 2	50.96	50.94	8.6	1.21	5 2 0	79.22	79.22	1.2
1.74	2 0 2	52.48	52.46	3.1					

octahedra in $Ba_3Ti_3O_6(BO_3)_2$ are largely distorted, giving the 0.02 nm off-center shift of the Ti^{4+} cations in TiO_6 octahedra. It is, therefore, considered that the TiO_6 octahedra in $Ba_3Ti_3O_6(BO_3)_2$ are highly polarizable units under the electric field of light. These structural features in the TiO_6 octahedral units would be one of the reasons that $Ba_3Ti_3O_6(BO_3)_2$ crystals show a strong SH intensity. It should be emphasized that both crystals of $BaTi(BO_3)_2$ and $Ba_3Ti_3O_6(BO_3)_2$ consist of TiO_6 octahedral units. The fact that these crystals are easily formed in the crystallization of $BaO–TiO_2–B_2O_3$ glasses with high TiO_2 contents (see in Table 1) suggests that some amounts of Ti^{4+} ions might be present as TiO_6 polyhedra in the glasses. Furthermore, the above discussion would support our interpretation of Raman scattering spectra shown in Fig. 2: the peak at $\sim 620\,cm^{-1}$ in the glasses with high TiO_2 contents corresponds to the formation of TiO_6 octahedra.

As seen in Fig. 5, $BaTi(BO_3)_2$ has some strong peaks at 1000–1250 cm^{-1}. These peaks are contributed by BO_3 triangles [39]. Although BO_3 units are present in both crystals of $BaTi(BO_3)_2$ and $Ba_3Ti_3O_6(BO_3)_2$ [6,26], $Ba_3Ti_3O_6(BO_3)_2$ shows an extremely weak peak at $1268\,cm^{-1}$. As proposed by Chen et al. [40], the degree of optical nonlinearity in borate crystals is strongly correlated with the type of B–O anionic molecules. Further experiments would be needed to clarify the contribution of BO_3 units on SH intensities of $BaTi(BO_3)_2$ and $Ba_3Ti_3O_6(BO_3)_2$ crystals.

3.5. Crystallization behavior of glasses

Since both $BaTi(BO_3)_2$ and $Ba_3Ti_3O_6(BO_3)_2$ crystals are nonlinear optical crystals, it is of interest to prepare transparent crystallized glasses consisting of these crystals. The glasses of $BaO–TiO_2–B_2O_3$ prepared in the present study were heat-treated at the crystallization peak temperature for 3 h. The crystalline phases determined by XRD analysis are summarized in Table 1. As a general trend, it is seen that β-BaB_2O_4 crystals are mainly formed in the glasses with the TiO_2 content of 20 mol%. On the other hand, in the glasses containing TiO_2 contents of over 30 mol%, the formation of $BaTi(BO_3)_2$ and $Ba_3Ti_3O_6(BO_3)_2$ crystals is confirmed. In the paper reported by Bhargava et al. [29], the formation of $BaTi(BO_3)_2$ crystals has been found, but $Ba_3Ti_3O_6(BO_3)_2$ crystals have not been detected. The crystalline phases shown in Table 1 are for the samples that were heat-treated at the crystallization peak temperature (T_p) for 3 h. According to the phase relations in the $BaO–TiO_2–B_2O_3$ system reported by Zhang et al. [36], other crystalline phases such as Ba_2TiO_4, $BaTiO_3$ and $BaTi_4O_9$ are formed in the sintered (solid-state reaction at 750–1050 °C for 48 h) samples. It is, therefore, expected that the crystallization of $BaO–TiO_2–B_2O_3$ glasses at higher temperatures ($> T_p$) would give additional crystalline phases.

The powder and bulk XRD patterns for the crystallized samples of $33.3BaO \cdot 33.3TiO_2 \cdot 33.3B_2O_3$ (Sample #7) are shown in Fig. 6. All peaks are assigned to $BaTi(BO_3)_2$ crystals, indicating that only the $BaTi(BO_3)_2$ phase is formed during crystallization. The composition of $33.3BaO \cdot 33.3TiO_2 \cdot 33.3B_2O_3$ corresponds to that of the $BaTi(BO_3)_2$ phase. It is evident that the crystallization of $33.3BaO \cdot 33.3TiO_2 \cdot 33.3B_2O_3$ glass will lead to the crystallization of the $BaTi(BO_3)_2$ phase. As seen in Fig. 6, the crystallized sample obtained by heat-treatment at 640 °C for 3 h has the strong peaks assigned to the (00*l*) planes compared with those in other crystallized (at 650 and 670 °C) samples, indicating that some amounts of $BaTi(BO_3)_2$ crystals are oriented at the surface of crystallized glasses, i.e., *c*-axis orientation. Recently, Maciente et al. [41,42] examined the surface crystallization of $63BaO \cdot 11TiO_2 \cdot 26B_2O_3$ glass by using a technique of CO_2 laser irradiation and found a preferred orientation of $BaTi(BO_3)_2$ crystals at the surface. The polarization optical microphotograph for the surface of the sample heat-treated at 640 °C is shown in Fig. 7. It is seen that sphere particles are observed. From the micro-Raman scattering spectra shown in Fig. 7, it is obvious that these particles are $BaTi(BO_3)_2$ crystals. The samples heat-treated at 640, 650 and 670 °C were unfortunately translucent. We applied a two-step heat-treatment method [43], i.e., the first step is for nucleation and the second step is for crystal growth, to $33.3BaO \cdot 33.3TiO_2 \cdot 33.3B_2O_3$ glass. At this moment, however, transparent crystallized glasses consisting of a

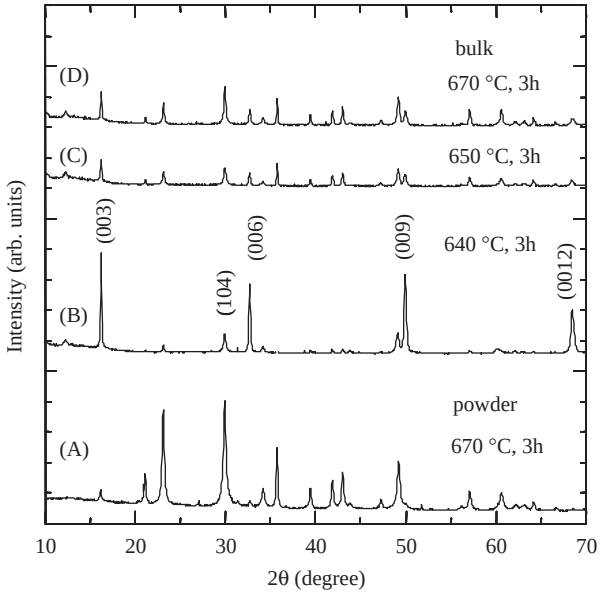

Fig. 6. XRD patterns for the crystallized glasses obtained by heat-treatments at 640, 650, and 670 °C for 3 h in $33.3BaO \cdot 33.3TiO_2 \cdot 33.3B_2O_3$ glass. The peaks are assigned to the $BaTi(BO_3)_2$ phase.

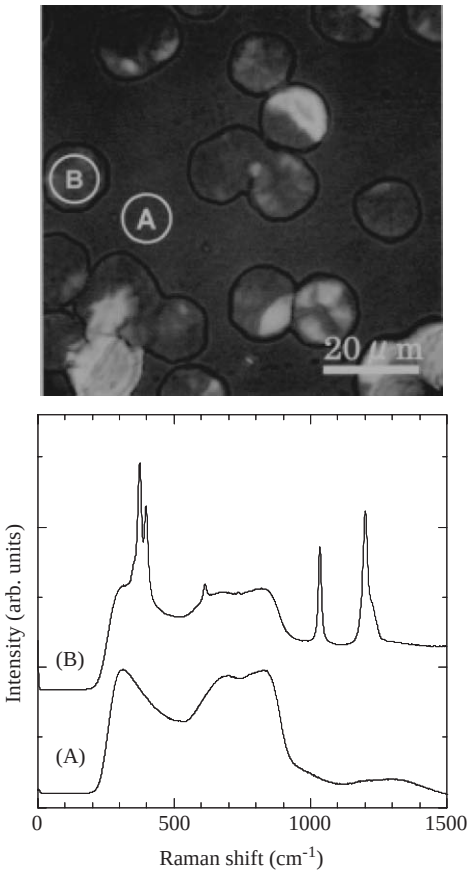

Fig. 7. Polarization optical microphotograph and microRaman scattering spectra for the surface of the sample heat-treated at 640 °C in $33.3BaO \cdot 33.3TiO_2 \cdot 33.3B_2O_3$ glass. (A) is the glassy part and (B) is a crystal part.

large amount of $BaTi(BO_3)_2$ crystals have not been successfully fabricated.

Ding et al. [44,45] developed a new procedure for enhanced nucleation and stimulated precipitation of desired crystal at a glass surface due to ultrasonic surface treatment (UST) of glass with suspensions containing crystalline particles. For instance, they succeeded in fabricating surface crystallized glasses with the *c*-axis orientation of optical nonlinear $Ba_2TiSi_2O_8$ crystals using a UST technique. In this study, we applied a UST technique to $33.3BaO \cdot 33.3TiO_2 \cdot 33.3B_2O_3$ glass. That is, first this glass was hold for 60 min in a suspension solution (~25 °C) containing $BaTi(BO_3)_2$ fine crystal powders under the ultrasonic treatment (frequency: 40 kHz), and after drying, the glass was heat-treated at 635 °C for 3 h in an electric furnace. The polarization optical microphotographs for the sample are shown in Fig. 8. It is seen that certainly the UST technique is very effective in enhancing nucleation at the surface of the glass. This sample is still translucent as shown in Fig. 8. More controlled heat-treatments are needed to fabricate transparent crystallized glasses with

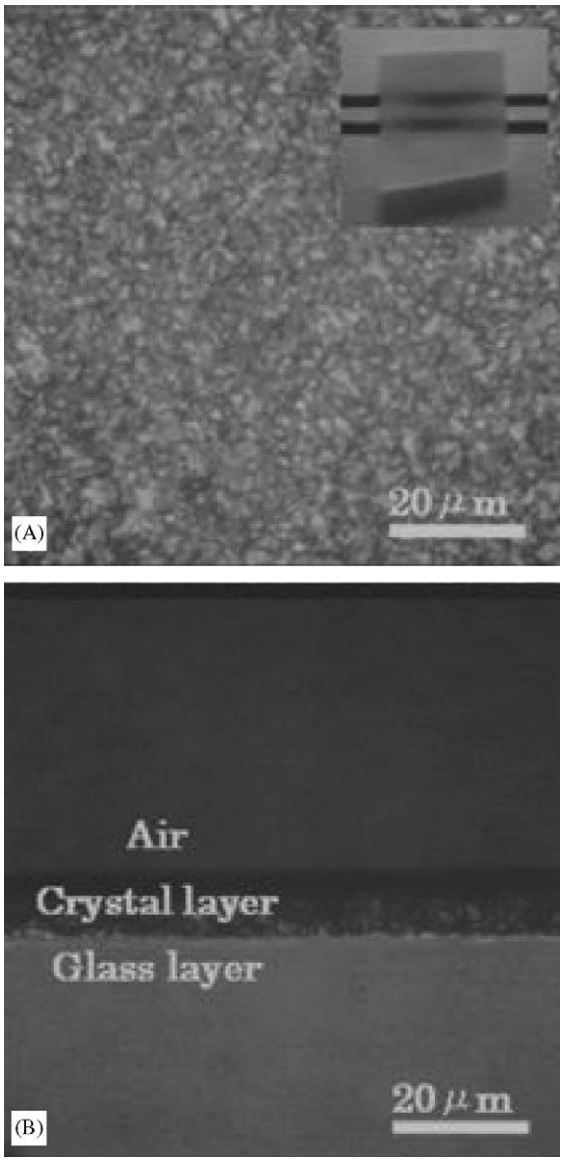

Fig. 8. Polarization optical microphotographs for the crystallized glass obtained by a ultrasonic surface treatment and usual heat-treatment (635 °C, 3 h) in $33.3BaO \cdot 33.3TiO_2 \cdot 33.3B_2O_3$ glass. (A) and (B) are top and cross-section views, respectively.

$BaTi(BO_3)_2$ crystals in $33.3BaO \cdot 33.3TiO_2 \cdot 33.3B_2O_3$ glass.

The SH intensity of the fully crystallized powder samples (heat-treated at 670 °C for 3 h) consisting of only $BaTi(BO_3)_2$ crystals was measured, and it was found to be approximately 0.8 times as large as α-quartz powders, i.e., $I^{2\omega}(\text{sample})/I^{2\omega}(\alpha-\text{quartz}) = 0.8$. This value is almost the same as that for $BaTi(BO_3)_2$ crystals synthesized by a solid-state reaction.

The powder and bulk XRD patterns for the crystallized sample (heat-treated at 740 °C for 3 h) of $40BaO \cdot 40TiO_2 \cdot 20B_2O_3$ (Sample #10) are shown in Fig. 9. The main crystalline phase is $Ba_3Ti_3O_6(BO_3)_2$. The formation of $BaTi(BO_3)_2$ crystals is also confirmed, although

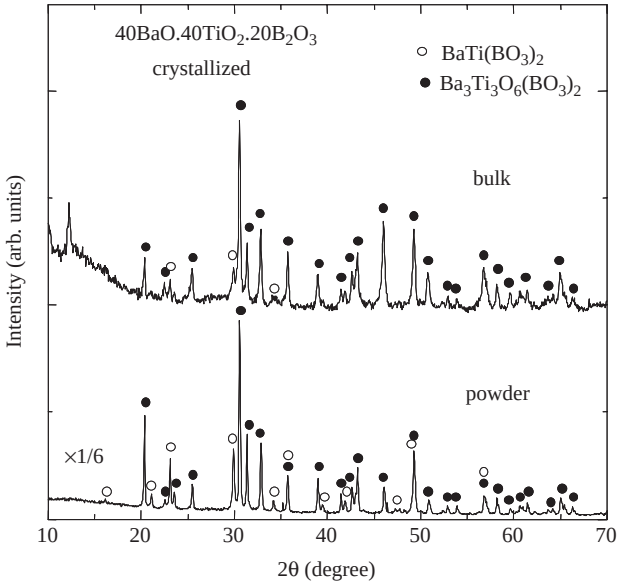

Fig. 9. Bulk and powder XRD patterns for the crystallized glass obtained by heat-treatment at 740 °C for 3 h in $40BaO \cdot 40TiO_2 \cdot 20B_2O_3$ glass.

the peak intensities in XRD patterns are small. In other crystallized samples obtained by heat-treatments of 630–800 °C, the formation of $Ba_3Ti_3O_6(BO_3)_2$ crystals was always confirmed as a main crystalline phase. But, the crystallized samples were translucent. The crystallized glass (heat-treated at 740 °C for 3 h) of Sample #10 was found to show a strong SH intensity of ~55 times as large as the α-quartz powders, i.e., $I^{2\omega}(\text{sample})/I^{2\omega}(\alpha-\text{quartz}) = 55$. The sample obtained by heat-treatment at 740 °C for 24 h exhibited the SH intensity of $I^{2\omega}(\text{sample})/I^{2\omega}(\alpha - \text{quartz}) = 68$.

We tried to fabricate transparent crystallized glasses consisting of mainly $Ba_3Ti_3O_6(BO_3)_2$ crystals through various heat-treatments in other $BaO–TiO_2–B_2O_3$ glasses, but at this moment, we have not succeeded in developing such transparent crystallized glasses. The XRD patterns for the bulk-crystallized glasses (heat-treated at 640 °C, 3 h and 740 °C for 3 h) of $40BaO \cdot 30TiO_2 \cdot 30B_2O_3$ (Sample #6) are shown in Fig. 10. In the sample heat-treated at 640 °C, it is seen that $BaTi(BO_3)_2$ crystals at the surface are highly oriented. In the sample heat-treated at a temperature (740 °C) higher than the crystallization peak temperature ($T_p = 709\,^{\circ}C$), the formation of $Ba_3Ti_3O_6(BO_3)_2$ crystals is observed, but this sample is opaque. The results shown in Fig. 10, therefore, indicate that the initial crystalline phase in $BaO–TiO_2–B_2O_3$ glasses with high TiO_2 contents is $BaTi(BO_3)_2$ crystals and then $Ba_3Ti_3O_6(BO_3)_2$ crystals are formed through the reaction of $BaTi(BO_3)_2$ crystals and TiO_2 and BaO. This would be one of the reasons for the difficulty of the development of transparent crystallized samples consisting of $Ba_3Ti_3O_6(BO_3)_2$ crystals. However, more detailed study on the crystallization

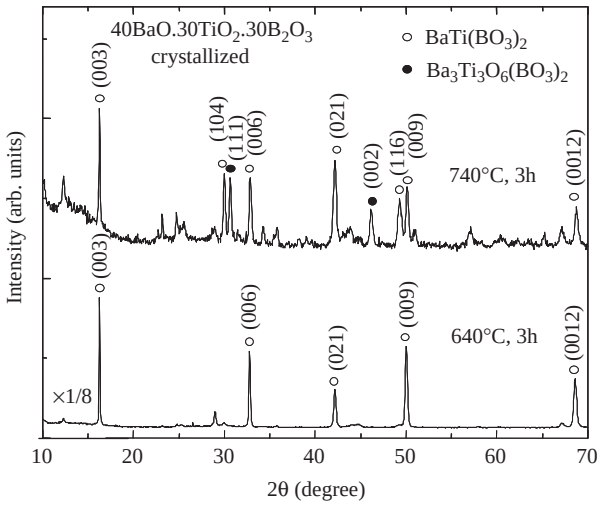

Fig. 10. Bulk XRD patterns for the crystallized glasses obtained by heat-treatments at 640 °C for 3 h and 740 °C for 3 h in $40BaO \cdot 30TiO_2 \cdot 30B_2O_3$ glass.

mechanism in the $BaO–TiO_2–B_2O_3$ glasses might give us some clues, e.g., suitable glass compositions or well-controlled heat-treatment steps, for the fabrication of transparent crystallized glasses. As indicated in the present study, it is difficult to prepare bulk glassy samples with the composition of $42.5BaO \cdot 42.5TiO_2 \cdot 15B_2O_3$ corresponding to $Ba_3Ti_3O_6(BO_3)_2$ using a conventional melt-quenching method. It is of interest to prepare thin films of $42.5BaO \cdot 42.5TiO_2 \cdot 15B_2O_3$ glass by using more rapid quenching techniques such as sputtering and to check their crystallization behaviors.

4. Conclusion

The ternary $BaO–TiO_2–B_2O_3$ glasses containing a large amount of TiO_2 (20–40 mol%) were prepared, and their optical basicities, the formation, structural features and second-order optical nonlinearities of $BaTi(BO_3)_2$ and $Ba_3Ti_3O_6(BO_3)_2$ crystals were examined to develop new nonlinear optical materials. The glasses with high TiO_2 contents of 30–40 mol% showed large optical basicities of $\Lambda = 0.81-0.87$, suggesting the high polarizability of TiO_n polyhedra ($n = 4-6$) in the glasses. It was found that $BaTi(BO_3)_2$ and $Ba_3Ti_3O_6(BO_3)_2$ crystals were formed as main crystalline phases in many glasses. The SH intensities of crystallized glasses were found to be 0.8 times as large as α-quartz powders, i.e., $I^{2\omega}(\text{sample})/I^{2\omega}(\alpha - \text{quartz}) = 0.8$, for the sample with $BaTi(BO_3)_2$ crystals and to be $I^{2\omega}(\text{sample})/I^{2\omega}(\alpha - \text{quartz}) = 68$ for the sample with $Ba_3Ti_3O_6(BO_3)_2$ crystals, indicating that both crystals are interesting nonlinear optical materials. The new XRD pattern for the $Ba_3Ti_3O_6(BO_3)_2$ phase was proposed through

Rietvelt analysis. The Raman scattering spectra for the $BaTi(BO_3)_2$ and $Ba_3Ti_3O_6(BO_3)_2$ crystals were measured for the first time, and the correlation between their SH intensity and structural features was discussed.

Acknowledgments

This work was supported from the SCOPE (Strategic Information and Communications R&D Promotion Program) project by the ministry of Public Management, Home Affairs, Posts and Telecommunications, Japan, from the Grant-in-Aid for Scientific Research from the Ministry of Education, Science, Sport, Culture, and Technology, Japan, and from the 21st Century Center of Excellence (COE) Program in Nagaoka University of Technology.

References

[1] Y. Takahashi, Y. Benino, T. Fujiwara, T. Komatsu, J. Appl. Phys. 89 (2001) 5282.
[2] G. Senthil, K.B.R. Varma, Y. Takahashi, T. Komatsu, Appl. Phys. Lett. 78 (2001) 4019.
[3] Y. Takahashi, Y. Benino, T. Fujiwara, T. Komatsu, Appl. Phys. Lett. 81 (2002) 223.
[4] Y. Takahashi, Y. Benino, T. Fujiwara, T. Komatsu, J. Appl. Phys. 95 (2004) 3503.
[5] K. Saito, Y. Takahashi, Y. Benino, T. Fujiwara, T. Komatsu, J. Ceram. Soc. Jpn. 112 (2004) S1257.
[6] H. Park, A. Bakhtiiarov, W. Zhang, I. Vargas-Baca, J. Barbier, J. Phys. Chem. Solids 177 (2004) 159.
[7] M. Imaoka, J. Ceram. Soc. Jpn. 69 (1961) 282.
[8] A. Bhargava, J.E. Shelby, R.L. Snyder, J. Non-Cryst. Solids 102 (1988) 136.
[9] E.M. Vogel, M.J. Weber, D.M. Krol, Phys. Chem. Glasses 32 (1991) 231.
[10] H. Nasu, T. Uchigaki, K. Kamiya, H. Kanbara, K. Kubodera, Jpn. J. Appl. Phys. 31 (1992) 3899.
[11] R. Adair, L.L. Chase, A.A. Payne, Phys. Rev. B 39 (1989) 3337.
[12] I.V. Kityk, A. Majchrowski, J. Ebothe, B. Sahraoui, Opt. Commun. 236 (2004) 123.
[13] S.K. Kurtz, T.T. Perry, J. Appl. Phys. 39 (1968) 3798.
[14] V. Dimitrov, S. Sakka, J. Appl. Phys. 79 (1996) 1736.
[15] V. Dimitrov, T. Komatsu, J. Non-Cryst. Solids 249 (1999) 160.
[16] V. Dimitrov, T. Komatsu, J. Ceram. Soc. Jpn. 107 (1999) 1012.
[17] V. Dimitrov, T. Komatsu, J. Ceram. Soc. Jpn. 108 (2000) 330.
[18] J.A. Duffy, Phys. Chem. Glasses 30 (1989) 1.
[19] J.A. Duffy, M.D. Ingram, J. Am. Chem. Soc. 93 (1971) 6448.
[20] J.A. Duffy, M.D. Ingram, J. Non-Cryst. Solids 21 (1976) 373.
[21] S. Matsumoto, T. Nanba, Y. Miura, J. Ceram. Soc. Jpn. 106 (1998) 415.
[22] T. Honma, R. Sato, Y. Benino, T. Komatsu, V. Dimitrov, J. Non-Cryst. Solids 272 (2000) 1.
[23] T. Honma, Y. Benino, T. Komatsu, R. Sato, V. Dimitrov, Phys. Chem. Glasses 43 (2002) 32.
[24] T. Honma, Y. Benino, T. Fujiwara, T. Komatsu, R. Sato, V. Dimitrov, J. Appl. Phys. 91 (2002) 2942.
[25] V. Dimitrov, T. Komatsu, Phys. Chem. Glasses 44 (2003) 401.
[26] J. Yamashita, T. Kurosawa, J. Phys. Soc. Jpn. 10 (1955) 610.
[27] V. Dimitrov, T. Komatsu, J. Solid State Chem. 163 (2002) 100.
[28] V. Dimitrov, T. Komatsu, J. Solid State Chem. 178 (2005) 831.
[29] A. Bhargava, R.L. Snyder, R.A. Condrare, Mater. Res. Bull. 22 (1987) 1603.
[30] T. Furukawa, W.B. White, Phys. Chem. Glasses 20 (1979) 69.
[31] S. Sakka, F. Miyaji, K. Fukumi, J. Non-Cryst. Solids 112 (1989) 64.
[32] S.T. Markgraf, S.K. Sharma, A.S. Bhalla, J. Am. Ceram. Soc. 75 (1992) 2630.
[33] S. Krimi, A. El Jazouli, L. Rabardel, M. Couzi, I. Mansouri, G. Le Flem, J. Solid State Chem. 102 (1993) 400.
[34] T. Cardinal, E. Fargin, G. Le Flem, M. Couzi, J. Solid State Chem. 120 (1995) 151.
[35] A. Tang, T. Hashimoto, T. Nishida, H. Nasu, K. Kamiya, J. Ceram. Soc. Jpn. 112 (2004) 496.
[36] S.Y. Zhang, X. Wu, X.L. Chen, M. He, Y.G. Cao, Y.T. Song, D.Q. Ni, Mater. Res. Bull. 38 (2003) 783.
[37] J.M. Millet, R.S. Roth, H.S. Parker, J. Am. Ceram. Soc. 69 (1986) 811.
[38] F. Izumi, T. Ikeda, Mater. Sci. Forum 198 (2000) 321.
[39] H.R. Xia, P. Zhao, X.F. Cheng, W.L. Liu, S.J. Zhang, Z.X. Cheng, Z.H. Yang, J. Appl. Phys. 95 (2004) 5383.
[40] C. Chen, Y. Wu, R. Li, J. Cryst. Growth 99 (1990) 790.
[41] A.F. Maciente, V.R. Mastelaro, A.L. Martinez, A.C. Hernandes, C.A.C. Carneiro, J. Non-Cryst. Solids 306 (2002) 309.
[42] A.F. Maciente, V.R. Mastelaro, A.L. Martinez, A.C. Hernandes, C.A.C. Feitosa, J. Non-Cryst. Solids 318 (2002) 331.
[43] K. Shioya, T. Komatsu, H.G. Kim, R. Sato, K. Matusita, J. Non-Cryst. Solids 189 (1995) 16.
[44] Y. Ding, A. Osaka, Y. Miura, J. Am. Ceram. Soc. 77 (1994) 749.
[45] Y. Ding, N. Masuda, Y. Miura, A. Osaka, J. Non-Cryst. Solids 203 (1996) 88.